Received: 21 November 2019 | Revised: 9 January 2020 | Accepted: 13 January 2020

DOI: 10.1002/pol.20190200

ORIGINAL ARTICLE

JOURNAL OF POLYMER SCIENCE WILEY

# Dual Stimuli-Responsive Self-Assembly Behavior of a Tailor-Made ABC-Type Amphiphilic Tri-Block Copolymer

**Sanjay Pal**[1] | **Michael Kather**[2,3] | **Sovan Lal Banerjee**[1] | **Pabitra Saha**[2,3] | **Andrij Pich**[2,3] | **Nikhil K. Singha**[1]

[1]Rubber Technology Centre, Indian Institute of Technology Kharagpur, Kharagpur, 721302, India

[2]DWI-Leibniz Institute for Interactive Materials, RWTH Aachen University, Aachen, 52074, Germany

[3]Institute of Technical and Macromolecular Chemistry, RWTH Aachen University, Aachen, 52074, Germany

**Correspondence**
N. K. Singha
E-mail: nks8888@yahoo.com and A. Pich
E-mail: pich@dwi.rwth-aachen.de

**Funding information**
Indian Institute of Technology Kharagpur; DWI, RWTH Aachen University, Germany; DST-DFG; German Academic Exchange Services (DAAD)

**Abstract**

This investigation describes the synthesis of a dual stimuli-responsive, amphiphilic ABC tri-block copolymer (BCP) based on the functional monomers via RAFT polymerization. In this case, ABC-type BCP was prepared based on *N*-isopropylacrylamide, *n*-butyl acrylate, and 4-vinylpyridine in DMF solvent using cyanomethyl dodecyl trithiocarbonate as the RAFT agent and azobisisobutyronitrile as a thermal initiator in a subsequent macro-RAFT approach, respectively. The BCPs were characterized by SEC, $^1$H-NMR, FTIR spectroscopy, and DSC analyses. Temperature and pH-dependent properties of the smart BCP micelles in aqueous medium were investigated using dynamic light scattering. Transmission electron microscopic images were taken at cryogenic and dry conditions to study the morphology of molecular assemblies of block copolymers in an aqueous medium. The phase and topographical images were captured by atomic force microscopy to understand the assembly of block copolymers in solvents of different polarities. The morphology of BCP micelles was transformed from flower-like to spherical in the presence of solvents with different polarities ($H_2O$ or $CHCl_3$).

**KEYWORDS**

amphiphilic block copolymer, dual stimuli-responsive, PNIPAM, RAFT polymerization, self-assembly

## 1 | INTRODUCTION

Nowadays, stimuli-responsive polymers are widely studied due to their unique behavior in the presence of external stimuli like temperature, pH, ionic strength, and so forth. In the presence of the external stimuli, responsive polymers can configure themselves in a wide variety of orientations, including spherical, lamellar, cylindrical vascular, and many more.[1–4] The upgradation of the polymeric structure to special orientations allows the polymeric architecture to be used in smart applications like membranes,[5,6] controlled drug delivery systems in biomedical applications,[7] tissue engineering,[8] electronics, optics, environmental or energy domain or polymeric coatings,[9] which is not possible for the linear analogous.

The highly cooperative interactions cause the nonlinear responses of the stimuli-responsive polymer. Each particular interaction taking place in a separate monomer unit is weak but additive in nature. So, a significant summation of the properties is expected in the presence of external stimuli

when the monomeric units are polymerized. Since the changes in temperature and pH are relatively simple to control, and also easily applicable, temperature and pH are the most widely used triggers in stimuli-responsive polymer systems. Typical thermoresponsive polymers are based on *N*-isopropylacrylamide (NIPAM),[10,11] *N,N*-diethylacrylamide,[12] methyl vinyl ether,[13] and *N*-vinylcaprolactam.[14] On the other hand, pH pH-responsive polymers are ionizable polymers with pKa values between 3 and 10.[15]

He and Shi et al. prepared and studied the effect of pH on the pyranine-induced micellization of poly(ethylene glycol)-*b*-poly(4-vinylpyridine) in aqueous solutions and pH-triggered release of pyranine from the complex micelles.[16] Shi et al. also studied the thermo- and pH-responsive micellization of poly(ethylene glycol)-*b*-poly (4-vinylpyridium) in water.[17] Zhu et al.[18] studied the effect of temperature and pH on the micelles PNIPAM-*b*-P4VP in an aqueous medium, which is considered to be a double responsive block copolymer (BCP). Dai et al. also report a similar system of a pH-induced reversible micellization.[19] Marty et al. recently studied the effect of copolymer composition of RAFT/MADIX-derived poly(*N*-vinylcaprolactam-*co*-*N*-vinylpyrrolidone) statistical copolymers on their thermoresponsive behavior and hydrogel properties.[20] In most of these studies of dual dual-responsive polymers, either AB-type di-block copolymers or ABC-type tri-block copolymers have been used. In that context, ABC-type smart BCPs would be an interesting material, as it can show not only dual-responsive properties but also multi-responsive properties. However, it needs challenging synthetic strategies to prepare tri- or n-block copolymers having asymmetric blocks or block lengths.

In this investigation, we reported for the first time RAFT-mediated synthesis of thermo- and pH-responsive poly(*N*-isopropylacrylamide-*b*-*n*-butylacrylate-*b*-4-vinylpyridine) (PNIPAM-*b*-PBA-*b*-P4VP), as ABC-type amphiphilic block copolymers using cyanomethyl dodecyl trithiocarbonate (CMDTTC) as RAFT agent and AIBN as an initiator. PNIPAM, being a thermoresponsive polymer, shows a LCST at around 32 °C, whereas. P4VP as a pH-sensitive polymer is soluble in water when the pH is less than 4.7 and becomes insoluble at higher pH values. PBA is chosen as a third block in the ABC-type tri-block copolymer to introduce a hydrophobic block, which reduces the volume phase transition temperature (VPTT) and improves low-temperature properties for the delivery of water-insoluble drugs. Due to its tackiness, it also reduces the minimum film-forming temperature to below room temperature. The micelles formed from such block copolymers in an aqueous medium can undergo various conformational changes, depending upon the different combinations of temperature and pH. In this work, the effect of solvent polarity on the self-assembly of BCP has also been studied using AFM technique. This amphiphilic BCP can act as a potential vehicle for various water-insoluble drugs in biomedical applications and coating applications on various surface systems due to the high tackiness of PBA.

## 2 | EXPERIMENTAL

### 2.1 | Materials

4-vinylpyridine (95%, 4-VP, Sigma-Aldrich), n-butyl acrylate (≥99%, BA, Sigma-Aldrich), and NIPAM (≥99% NIPAM, Sigma-Aldrich) monomers were purified via vacuum distillation before use. DMF, azobisisobutyronitrile (98%, AIBN, Sigma-Aldrich), and CMDTTC (≥99%, CMDTTC, Sigma-Aldrich) were used as received PNIPAM.

### 2.2 | Synthesis of PNIPAM Using CMDTTC as RAFT Agent

NIPAM (1 g, 8.85 mmol), CMDTTC (56.2 mg, 0.17 mmol), AIBN (3 mg, 0.017 mmol), and DMF (2.5 g, 34.2 mmol) were added to a Schlenk flask equipped with a magnetic stirrer. The solution was degassed by three freeze pump thaw (FPT) cycles and set under a nitrogen atmosphere. The reaction mixture was subsequently heated in an oil bath at 70 °C. Samples were periodically withdrawn from the polymerization medium for the determination of monomer conversion and molecular weights by SEC. The polymerization was stopped after 3 h by quenching it in liquid nitrogen ($M_n$ = 5220 g mol$^{-1}$, PDI = 1.05). The $^1$H-NMR of the PNIPAM macro-RAFT is discussed in Figure S1 and the presence of peak signals at 1680 (>C═O amide) and 3435 cm$^{-1}$ (—NH st.) in the FTIR spectrum of Figure 3 (a) show the formation of the PNIPAM macro-RAFT. Finally, the polymer was precipitated from a large volume of cold diethyl ether and the product was vacuum dried under reduced pressure at 50 °C. Using the same procedure, homopolymers of BA and 4-VP were also prepared for FTIR comparative study.

### 2.3 | Preparation of PNIPAM-*b*-PBA, AB-Type Block Copolymer

In a typical procedure, *n*-butyl acrylate (1 g, 7.8 mmol), PNIPAM macro-RAFT agent (0.81 g, 0.15 mmol), AIBN (2.6 mg, 0.016 mmol), and DMF (4 g, 54.8 mmol) were taken in a 25 mL Schlenk flask equipped with a magnetic stirrer (Scheme 1). The solution was degassed by three

FPT cycles and set under a nitrogen atmosphere. The polymerization process was carried out at 70 °C in an oil bath. The reaction was terminated after 3 h by quenching it in liquid nitrogen. The polymer was extracted from the reaction mixture by centrifugation in an aqueous medium and the extracted product was dialyzed with a 3500 kDa MWCO membrane for 3 d to get the pure product. Then, it was dried in a vacuum oven at 60 °C for 24 h. Comparing the NMR spectra of the homo- (Fig. S1) and di-block copolymer (Fig. S2), it can be seen that the peak intensity at 4.0 ppm increases in the copolymer, along with the appearance of new proton signals at 0.8–-2.5 ppm, confirming the successful addition of the PBA block.

## 2.4 | Preparation of PNIPAM-*b*-PBA-*b*-P4VP, ABC-Type Block Copolymer

In a typical procedure, 4-vinylpyridine (0.5 g, 4.7 mmol), PNIPAM-*b*-PBA (1.14 g, 0.09 mmol), AIBN (1.6 mg, 0.01 mmol), and DMF (4 g, 54.8 mmol) were taken in a Schlenk flask equipped with a magnetic stirrer (Scheme 1). The solution was degassed through three FPT cycles and set under a nitrogen atmosphere. The solution was then heated in an oil bath at 70 °C for 24 h. The polymerization was stopped by quenching it in liquid nitrogen. The polymer was extracted from the reaction mixture by centrifugation in an aqueous medium and the mass was dialyzed with a 10,000 kDa MWCO membrane for 3 d to receive the pure product. Afterward, it was dried in a vacuum oven at 60 °C for 24 h (see Fig. 3 FTIR spectra 1680 [>C═O amide] and 3435 $cm^{-1}$ [—NH st.] from PNIPAM, 1734 $cm^{-1}$ [>C═O ester] and 1597 $cm^{-1}$ [C═C bending of aromatic ring] from P4VP).

## 2.5 | Characterization Techniques

### 2.5.1 | Gel Permeation Chromatography

Molecular weights and dispersity of the polymers were measured by a combined GPC system equipped with a high-performance liquid chromatography pump (Bischoff HPLC), a Jasco 2035-plus RI detector, and four MZ-DVB gel columns (30, 100, and 2 × 3000 Å) in series. A solution of DMF containing 1.0 g $L^{-1}$ LiBr was used as eluent (flow: 1.0 mL $min^{-1}$). The molecular weights were calculated using a poly(styrene) (PS) calibration.

### 2.5.2 | Nuclear Magnetic Resonance

$^1$H-NMR spectra of the copolymer in $CDCl_3$ were recorded on a Bruker DPX-400 FT NMR operating at 400 MHz.

### 2.5.3 | Fourier-Transform Infrared

FTIR spectra (resolution 4 $cm^{-1}$) of homo- and co-polymers were recorded using a Nicolet NEXUS 670 FTIR spectrometer. Samples were tested under ATR mode. For each spectrum, more than 200 scans were averaged to enhance the signal-to-noise ratio.

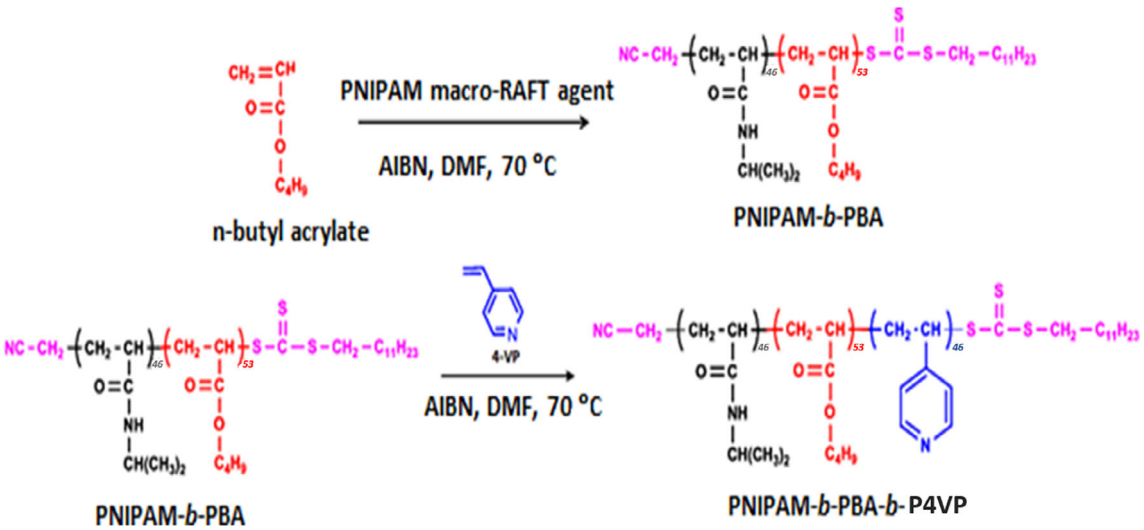


**SCHEME 1** The schematic reaction for the synthesis of PNIPAM-*b*-PBA-*b*-P4VP tri-block copolymer [Color figure can be viewed at wileyonlinelibrary.com]

### 2.5.4 | Transmission Electron Microscopic

A JEOL USA JEM-2100F TEM was used under cryo conditions. The electron beam accelerating voltage was set at 200 kV. Analytical TEM images were taken using the FEI Tecnai™ electron microscope (made in the Czech Republic) at 120 kV electron beam accelerating voltage. Ten microliters of 0.2 mg $mL^{-1}$ aqueous solution of BCP was trickled on a piece of Formvar carbon-coated copper grid, which was cooled to −150 °C with the help of liquid nitrogen for cryo-TEM analysis, otherwise, for analytical TEM, the images were taken at 20 °C.

### 2.5.5 | Atomic Force Microscopy

Intermittent contact mode atomic force microscopy (AC-AFM) (Agilent 5500 Scanning Probe Microscope) with a tip resonance frequency varying from 146 to 236 Hz and 48 N $m^{-1}$ force constant was used to study the phase morphology and topography of the BCP. Two 5 mg $mL^{-1}$ BCP solutions were prepared separately in analytical grade $H_2O$ (99%) and $CHCl_3$ (99%) solvent: A 50 μL drop of BCP solution was placed over the clean microscopic glass slide and dried in a vacuum oven at 60 °C for 3 h. Sample coated glass slides were then taken to record the AFM images.

### 2.5.6 | Dynamic Light Scattering

Temperature-dependent changes in the hydrodynamic radius of the micelles formed in an aqueous medium were measured with a DLS spectrometer (ALV DLS/SLS-5000) equipped with an ALV-5000/EPP multiple tau digital correlator and laser goniometry system-ALV/CGS-8F S/N 025 with a helium-neon laser (Uniphase 1145P, output power of 21 mW and wavelength of 632.8 nm) as a light source at 90° scattering angle. The acquisition time was set for 90 s. Based on the data available in the literature,[18] the critical micelle concentration of similar BCP lies at 0.01 mg $mL^{-1}$. Therefore, the PNIPAM-*b*-PBA-*b*-P4VP copolymer was dissolved in acidic water (pH 3) to prepare an aqueous solution with a concentration of 0.2 mg $mL^{-1}$. The solution was passed through a 0.2 μm PET-filter into a clean vial to avoid multiple scattering by impurities. The measurements were performed at a series of temperatures varied from 10 to 45 °C. A similar procedure was repeated to compare the effect of temperature on the hydrodynamic radius of micelles at pH 8.

### 2.5.7 | Differential Scanning Calorimetry

A DSC 200 F3 Maia thermal analyzer (Netzsch-Gerätebau GmbH) was used to measure various thermal transitions at a 10 °C $min^{-1}$ scanning rate between −150 and 200 °C. Approximately 10 mg of the sample was taken on the aluminum crucibles for thermal analysis.

## 3 | RESULTS AND DISCUSSION

ABC-type BCP, i.e. PNIPAM-*b*-PBA-*b*-P4VP, was prepared sequentially, as shown in Scheme 1. In this case, PNIPAM macro-RAFT agent was initially prepared via RAFT polymerization, followed by the preparation of PNIPAM-*b*-PBA, that is, AB-type BCP. Finally, the ABC-type BCP was prepared using PNIPAM-*b*-PBA as a macro-RAFT agent. In each step, homopolymer and copolymers were characterized by GPC, $^1$H-NMR, and FTIR analyses. Figure 1 shows the SEC traces of homopolymer, AB-di-block, and ABC-tri-block copolymer. A gradual shift of the SEC traces for homopolymer, di-block, and tri-block copolymer toward higher molecular weights, or lower retention time indicates the formation of BCP in each step.

Table 1 summarizes the average molecular weight and dispersity of the different polymers. The theoretical molecular weight was calculated by the given equation:

$$M_{n^{th}} = \text{Conversion}(\%)\left(\frac{[M^\circ]}{[CTA]}\right)M_m + M_{(CTA)} \quad (1)$$

where ([M°]/[CTA]) is the molar ratio between monomer (M°) and chain transfer agent (CTA) in the feed, and $M_m$ and $M_{CTA}$ are the molar masses of the monomer and CTA, respectively.

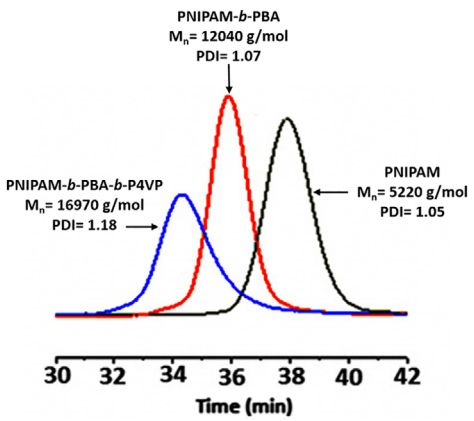


**FIGURE 1** GPC traces of different macro-RAFT-mediated homopolymer and block copolymers [Color figure can be viewed at wileyonlinelibrary.com]

**TABLE 1** Summary of the Molecular Weights of PNIPAM Macro-RAFT, AB, and ABC Block Copolymers

| S. No. | Samples | Molar ratio $[M_0]$:[CTA]:[I] | Time (h) | Conversion (%) | $M_{n,Theo}$ (g mol$^{-1}$) | $M_{n,GPC}$ (g mol$^{-1}$) | Dispersity ($D$) |
|---|---|---|---|---|---|---|---|
| 1 | PNIPAM | 45:1:0.1 | 3 | 87 | 5100 | 5220 | 1.05 |
| 2 | $(PNIPAM)_{46}$-*b*-$(PBA)_{53}$[a] | 50:1:0.1 | 3 | 90 | 11,500 | 12,040 | 1.07 |
| 3 | $(PNIPAM)_{46}$-*b*-$(PBA)_{53}$-*b*-$(P4VP)_{46}$[b] | 46:1:0.1 | 24 | 94 | 16,400 | 16,970 | 1.18 |

[a]This AB-type block copolymer was prepared using PNIPAM ($M_n$ = 5220 g mol$^{-1}$) as the macro-RAFT agent.
[b]This ABC-type block copolymer was prepared using PNIPAM-*b*-PBA ($M_n$ = 12,040 g mol$^{-1}$) as the macro-RAFT agent.

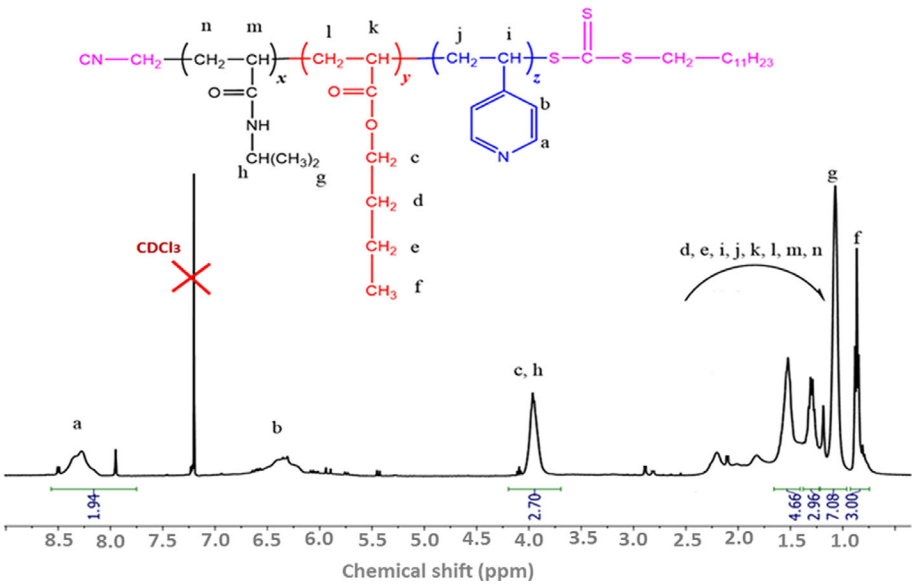


**FIGURE 2** $^1$H NMR spectra of the PNIPAM-*b*-PBA-*b*-P4VP block copolymer in $CDCl_3$ [Color figure can be viewed at wileyonlinelibrary.com]

The chemical structures of the homopolymer of NIPAM and its BCPs were elucidated using $^1$H-NMR spectra. The $^1$H-NMR spectrum of the PNIPAM homopolymer is shown in Fig. S1. The PNIPAM segment shows a characteristic resonance peak at 3.94 ppm due to the proton of tertiary carbon (>CH—, h). Figure 2 shows the $^1$H-NMR spectrum of PNIPAM-*b*-PBA-*b*-P4VP copolymer recorded in $CDCl_3$ solvent. The presence of the PBA segment in the tri-block copolymer was confirmed through the presence of characteristics resonances at 0.99 ppm (—$CH_3$, f), 2.20 ppm (>$CH_2$, d), and at 4.05 ppm (—$OCH_2$—, c). Whereas the presence of the resonance peak at 8.30 ppm (>$CH_2$, a) is due to the aromatic protons of P4VP, which confirms its presence in the BCP.

Figure 3(a) shows the FTIR spectra for the P4VP, PBA, and PNIPAM homopolymers. Aromatic C—H stretching at 3030 cm$^{-1}$ and aromatic C=C bending at 1597 cm$^{-1}$ indicate the presence of the aromatic ring in the P4VP segment of BCP. Along with this, a peak at 1442 cm$^{-1}$ shows the presence of C=N stretching vibration of the P4VP segment. PBA and PNIPAM show characteristic vibrational peaks at 1734 cm$^{-1}$ (>C=O stretch) and 3435 cm$^{-1}$ (amide —NH— stretch), respectively. The IR spectra shown in Figure 3(b) depict all the characteristic peaks of PNIPAM, PBA, and P4VP homopolymers, which confirm the structure of the PNIPAM-*b*-PBA-*b*-P4VP tri-block copolymer.

## 3.1 | Self-Assembly Behavior of pH and Thermo-Responsive BCP

The change in the hydrodynamic radius of the BCP micelles in an aqueous solution was measured as a function of temperature at different pH (3 and 8) in DLS method and the results are shown in Fig. 4. Variation of the temperature at pH 3 resulted in a change in the hydrodynamic radius of the micelles. The decrease in the BCP particle size (42–31 nm) with an increase in temperature can be described by considering the thermoresponsiveness of the PNIPAM segment [Fig. 4(a)], where the collapse of PNIPAM chains above its LCST was restricted by the protonation of P4VP part at pH 3.

The addition of hydrophobic groups into a thermoresponsive polymer shifts the LCST toward lower temperatures.[21] This phenomenon could be observed when the

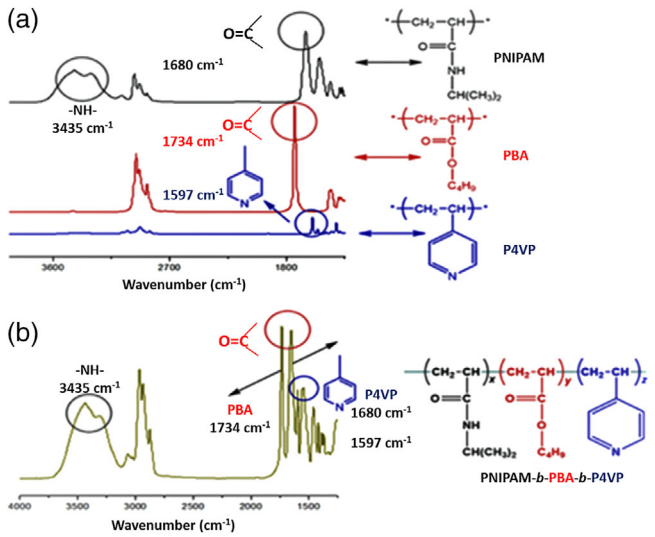


**FIGURE 3** FTIR spectra of different homopolymers and block copolymers in the wavenumber region between 1400 and 3500 $cm^{-1}$ for (a) P4VP, PBA, and PNIPAM homopolymers and (b) PNIPAM-*b*-PBA-*b*-P4VP block copolymer [Color figure can be viewed at wileyonlinelibrary.com]

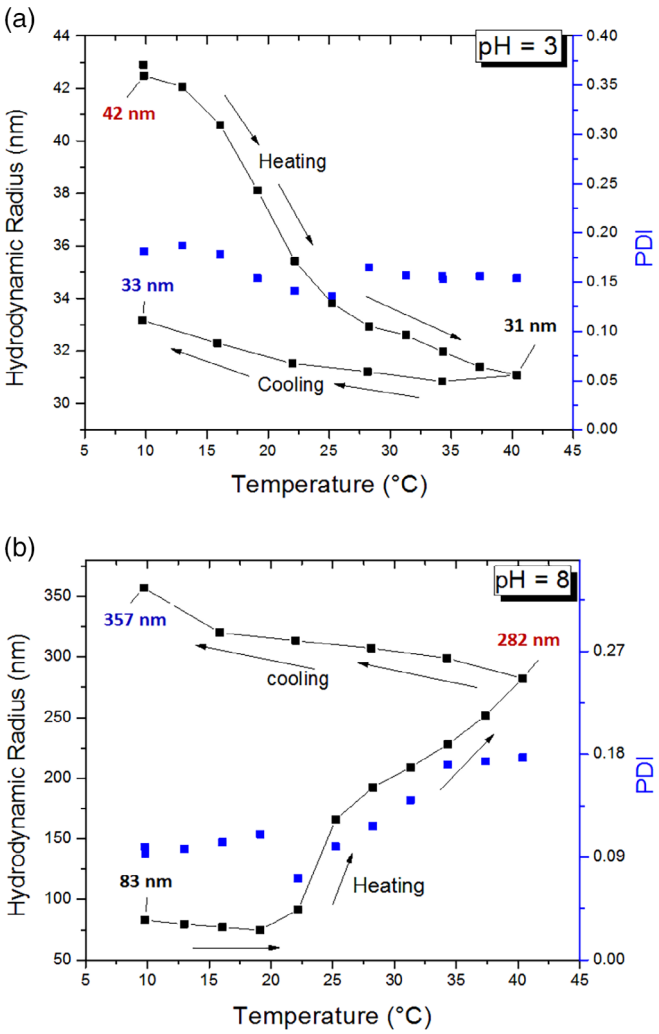


**FIGURE 4** Variation of the hydrodynamic radius and PDI of BCP micelles at different temperatures at (a) pH 3 and (b) pH 8 [Color figure can be viewed at wileyonlinelibrary.com]

higher hydrophobic PBA part helped the BCP micelles to self-aggregate at 24 °C (83–165 nm), which is lower than the VPTT of pure PNIPAM under basic condition (at pH 8). After that, a gradual increase in the particle size from 165 to 282 nm has been observed up to 45 °C [Fig. 4(b)]. Interestingly, the particle size increased from 282 to 357 nm during the cooling cycle. It is clear from Figure 4(b) that micelle in an aqueous medium at pH 8 could not re-disperse into smaller micelles and remained aggregated upon a decrease in temperature.

On the other hand, micelles at pH 3 showed some reversibility in hydrodynamic radius. This phenomenon can be seen as an analogy for the coagulation of natural rubber latex when colloidal particles become destabilized upon the loss of repulsive force between them.

At pH 8, both P4VP and PBA became hydrophobic in nature, so P4VP occupied the core position in the micelle and did not provide the repulsive force between micelles to prevent aggregation as it used to do in protonated condition at pH 3, thereby lost the reversible swelling/deswelling characteristics. At pH 8, along with the absence of positive charge, the formation of the intramolecular interaction between the PNIPAM segments of different BCP particles also accelerates the segregation while heating.

The particle size distribution index (PDI) of the micelles was also affected by the pH of the aqueous solution. At pH 3, the polydispersity of the micelles did not change significantly and was found within the range from 0.14 to 0.18 [Fig. 4(a)]. It implies that micelles did not coalesce, and their size and shape remained roughly identical throughout the temperature variation. However, at pH 8 the PDI value of the micelles was found rising from 0.07 to 0.20, after reaching the critical temperature [Fig. 4(b)]. This implies that the critical aggregation temperature of BCP seems to be influenced by the pH of the surrounding environment. Figure 5 shows the TEM image of the molecular assembly of BCP captured under cryogenic conditions (−150 °C) and at 25 °C and pH 8. A vesicle-type structure was observed when TEM images were taken at −150 °C, where the mean size of the micelle was found to be 35 ± 2 nm [Figure 5(a)], but at 25 °C, that is, above VPTT of BCP, the mean size of the micelle was dramatically increased (200 ± 10 nm) (Fig. 5) almost up to six-fold due to conformational changes caused by self-assembly.

The model shown in Scheme 2 illustrates the formation of micelles out of BCP at a temperature lower than

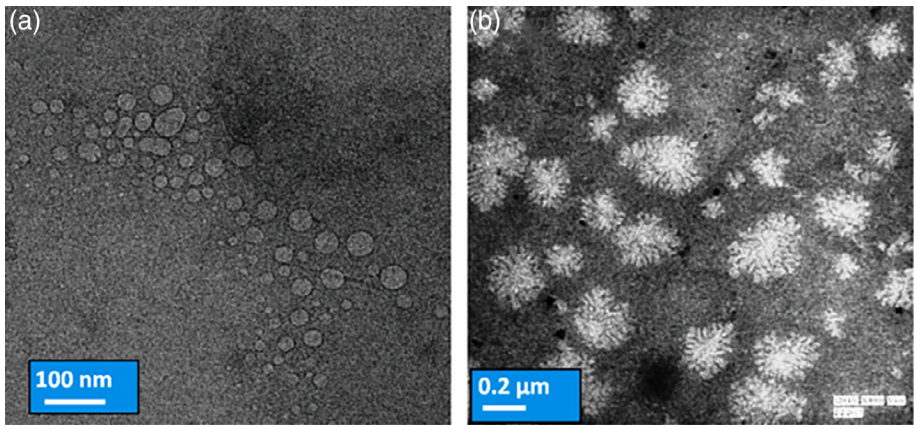


**FIGURE 5** TEM images for PNIPAM-*b*-PBA-*b*-P4VP micelles at pH 8, (a) at cryogenic condition (−150 °C), mean particle diameter = 35 nm (b) at 20 °C, mean particle diameter = 240 nm [Color figure can be viewed at wileyonlinelibrary.com]

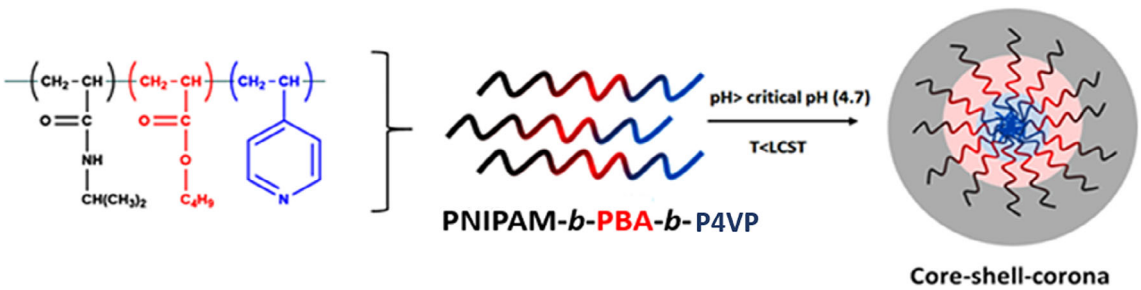


**SCHEME 2** Schematic representation of the conformational change of PNIPAM-*b*-PBA-*b*-P4VP [Color figure can be viewed at wileyonlinelibrary.com]

the LCST and at a pH value greater than 4.7, which supports the images obtained from TEM analysis. In order to understand the thermal transition behavior of a typical ABC-tri-block copolymer, DSC analysis of the prepared BCPs was carried out. Figure S2 shows the heating and cooling cycle thermogram of the amphiphilic ABC tri-block copolymer, indicating the multiple endothermic transitions and microphase crystallization of the tri-block copolymer. The soft-microphase, that is, PBA of the ABC tri-block copolymer exhibits a glass-transition temperature ($T_g$) at −49 °C and changes in heat capacity ($\Delta C_p$) at $T_g$ is 0.201 J/(g K). The DSC thermogram demonstrates the BCPs undergoing microphase separation transition in the form of an endothermic peak at ~100 °C. However, the cooling thermogram exhibits two distinct crystallization peaks at ~69 and 47 °C, indicating the formation of two different types of microphases (see Fig. S3).

The most important feature of the amphiphilic BCPs is the formation of self-assembled structures in the presence of solvents having distinctly different polarities. In the presence of a biphasic solvent, BCPs can configure themselves into different types of self-assembled structures such as spherical, cylindrical, star, or flower shape. Among a wide range of amphiphilic systems, linear amphiphilic BCPs cover up the center of attraction due to their self-assembly in the presence of a mixture of thermodynamically favorable and unfavorable solvents for specific segments of the BCP. Figure 6 shows the comparative phase morphology and topographical images of BCP using $H_2O$ at pH 8 and $CHCl_3$ as a solvent. In the given phase and topographical images, the yellowish region symbolizes the collapsed chain segment of the BCP, that is, PNIPAM or P4VP, and the dark-brown region represents the swollen segment, that is, PBA. The response of the thermoresponsive PNIPAM segment toward the solvent nature during phase development is quite evident from Figure 6(a,b). The use of the polar solvent $H_2O$ resulted in a star-shaped morphology, but BCP configured into an inter-diffused spherical type of morphology consisting of collapsed and swollen polymeric segments when the less polar solvent $CHCl_3$ was used. In the case of a water solution having a pH of 8, the PNIPAM segment occupied the outer segment of the self-assembled structure. Whereas, PBA and P4VP occupied the center part by formatting a compartmentalized core as discussed earlier. It has been reported that when the soluble block predominates over the insoluble block, it configured itself into a special kind of orientation like spherical, star-like, flower-like, depending on the nature of the polymer present on the BCP system.

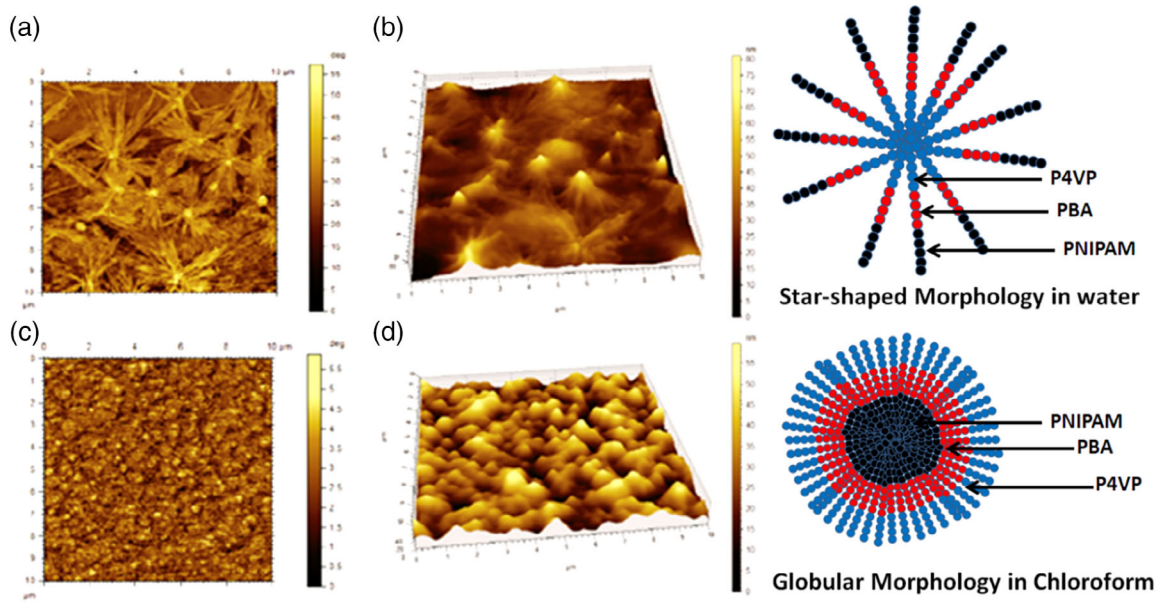


**FIGURE 6** AFM images of phase morphology (a, c) and topography (b, d) of drop cast film of BCP using aqueous solution of pH 8 (a, b) and $CHCl_3$ (c, d) [Color figure can be viewed at wileyonlinelibrary.com]

The presence of a molecular curvature formed due to the relative size of the hydrophilic and hydrophobic block provides significant influence over the formation of this kind of interesting morphologies.

The Hildebrand solubility parameter value for $H_2O$ is 48 $MPa^{1/2}$, whereas, in the case of $CHCl_3$ it is 18.7 $MPa^{1/2}$.[22] Due to this phenomenon, the hydrophobic segments are highly soluble in $CHCl_3$. In our system, due to the difference in polarity between more hydrophobic PBA and other two segments, that is, PNIPAM and P4VP, the system tries to orient them in a globular morphology where the presence of PBA and P4VP is expected in the shell position surrounding the PNIPAM core in $CHCl_3$ solvent.

## 4 | CONCLUSIONS

In conclusion, a thermo- and pH-responsive (dual-stimuli) amphiphilic BCP (PNIPAM-*b*-PBA-*b*-P4VP) was successfully synthesized via RAFT polymerization. Various spectroscopic techniques and SEC measurements confirmed the structure and narrow dispersity of ABC-type amphiphilic block copolymers. The micelles of such amphiphilic BCPs showed an interesting assembly transformation upon a change in temperature and pH in an aqueous medium, as shown by DLS measurements. TEM images taken under cryogenic and normal conditions clearly showed the temperature-dependent molecular association of the BCP. Furthermore, from the AFM images, it was explained that the molecular association of BCPs also depends on the nature of the solvent. Using this simple procedure, such BCPs can be further tailored to match specific requirements in applications such as controlled drug delivery, biomedical engineering, and environmental or energy domain.

## ACKNOWLEDGMENTS

Sanjay Pal cordially acknowledges the financial support from German Academic Exchange Services (DAAD) through the IIT sandwich fellowship program. Nikhil K. Singha and Andrij Pich acknowledge DST-DFG for financial assistance via funding a project under the Indo-German academic exchange program. The state-of-the-art research facility at DWI, RWTH Aachen University, Germany, and Indian Institute of Technology Kharagpur, India are also greatly acknowledged. P. Siva, IIT Kharagpur is acknowledged for his assistance in this work.

## REFERENCES

[1] S. K. Ahn, R. M. Kasi, S.-C. Kim, N. Sharma, Y. Zhou, *Soft Matter* **2008**, *4*, 1151.

[2] C. L. McCormick, S. E. Kirkland, A. W. York, *J. Macromol. Sci., Part C: Polym. Rev.* **2006**, *46*, 421.

[3] S. Minko, *J. Macromol. Sci., Part C: Polym. Rev.* **2006**, *46*, 397.

[4] T. R. Hoare, D. S. Kohane, *Polymer* **2008**, *49*, 1993.

[5] K. B. Doorty, T. A. Golubeva, A. V. Gorelov, Y. A. Rochev, L. T. Allen, K. A. Dawson, W. M. Gallagher, A. K. Keenan, *Cardiovasc. Pathol.* **2003**, *12*, 105.

[6] S. Wilson, A. Gorelov, Y. Rochev, F. McGillicuddy, K. Dawson, W. Gallagher, A. Keenan, *J. Biomed. Mater. Res. A* **2003**, *67*, 667.

[7] T. Shimoboji, E. Larenas, T. Fowler, A. S. Hoffman, P. S. Stayton, *Bioconjug. Chem.* **2003**, *14*, 517.

[8] J. P. Vacanti, R. Langer, *Lancet* **1999**, *354*, S32.
[9] M. A. C. Stuart, W. T. Huck, J. Genzer, M. Müller, C. Ober, M. Stamm, G. B. Sukhorukov, I. Szleifer, V. V. Tsukruk, M. Urban, *Nat. Mater.* **2010**, *9*, 101.
[10] H. G. Schild, *Prog. Polym. Sci.* **1992**, *17*, 163.
[11] T. Motonaga, M. Shibayama, *Polymer* **2001**, *42*, 8925.
[12] M. Kobayashi, S. Okuyama, T. Ishizone, S. Nakahama, *Macromolecules* **1999**, *32*, 6466.
[13] L. M. Mikheeva, N. V. Grinberg, A. Y. Mashkevich, V. Y. Grinberg, L. T. M. Thanh, E. E. Makhaeva, A. R. Khokhlov, *Macromolecules* **1997**, *30*, 2693.
[14] Y. C. Yu, G. Li, J. Kim, J. H. Youk, *Polymer* **2013**, *54*, 6119.
[15] R. A. Siegel, *Handbook of Advances in Polymer Science*; Springer: Berlin, Heidelberg, **1993**; Vol. 109, p. 233.
[16] R. Ma, B. Wang, X. Liu, Y. An, Y. Li, Z. He, L. Shi, *Langmuir* **2007**, *23*, 7498.
[17] K. Wu, L. Shi, W. Zhang, Y. An, X. Zhang, Z. Li, X. Zhu, *Langmuir* **2006**, *22*, 1474.
[18] Y. Xu, L. Shi, R. Ma, W. Zhang, Y. An, X. Zhu, *Polymer* **2007**, *48*, 1711.
[19] S. Dai, P. Ravi, K. C. Tam, B. Mao, L. Gan, *Langmuir* **2003**, *19*, 5175.
[20] X. Zhao, O. Coutelier, H. H. Nguyen, C. Delmas, M. Destarac, J. D. Marty, *Polym. Chem.* **2015**, *6*, 5233.
[21] P. Saha, M. Kather, S. L. Banerjee, N. K. Singha, A. Pich, *Eur. Polym. J.* **2019**, *118*, 195.
[22] A. Y. Kwok, G. G. Qiao, D.H. Solomon, *Polymer.* **2004**, *45*, 4017.

## SUPPORTING INFORMATION

Additional supporting information may be found online in the Supporting Information section at the end of this article.

**How to cite this article:** Pal S, Kather M, Banerjee SL, Saha P, Pich A, Singha NK. Dual Stimuli-Responsive Self-Assembly Behavior of a Tailor-Made ABC-Type Amphiphilic Tri-Block Copolymer. *J Polym Sci*. 2020;58:843–851. https://doi.org/10.1002/pol.20190200